Methane fluxes from arctic & boreal North America: Comparisons between process-based estimates and atmospheric observations

Hanyu Liu[1], Felix R. Vogel[5], Misa Ishizawa[5], Zhen Zhang[4], Benjamin Poulter[7], Doug E.J. Worthy[5], Leyang Feng[1], Anna Laure Gagné-Landmann[3], Ao Chen[1], Ziting Huang[1], Dylan C. Gaeta[1], Joe R. Melton[6], Douglas Chan[5], Vineet Yadav[2], Deborah Huntzinger[3], and Scot M. Miller[1]

[1] Department of Environmental Health and Engineering, Johns Hopkins University, Baltimore, MD, USA
[2] Jet Propulsion Laboratory, California Institute of Technology, Pasadena, CA, USA
[3] School of Earth and Sustainability, Northern Arizona University, Flagstaff, AZ, USA
[4] Institute of Tibetan Plateau Research, Chinese Academy of Sciences, Beijing, China
[5] Environment and Climate Change Canada, Toronto, ON, Canada
[6] Environment and Climate Change Canada, Victoria, BC, Canada
[7] National Aeronautics and Space Administration, Greenbelt, MD, USA

INTRODUCTION

- Rising temperatures and permafrost thaw create more opportunities for methanogens to produce methane under anaerobic conditions, contributing to a positive climate feedback in Arctic-boreal regions.
- Existing process-based models can lead to uncertainties in the magnitude, seasonality, and spatial distribution of CH_4 fluxes across high-latitude America.

RESEARCH QUESTIONS

1. **Model Evolution: How have process-based CH_4 flux models progressed over time?**
2. **Model–Observation Comparison: How well do global-scale process-based models capture the magnitude of CH_4 fluxes compared to atmospheric observations in high-latitude North America?**
3. **Spatial–Temporal Patterns: What spatial-temporal patterns are commonly observed in models that closely align with atmospheric measurements?**

GLOBAL CARBON PROJECT MODEL

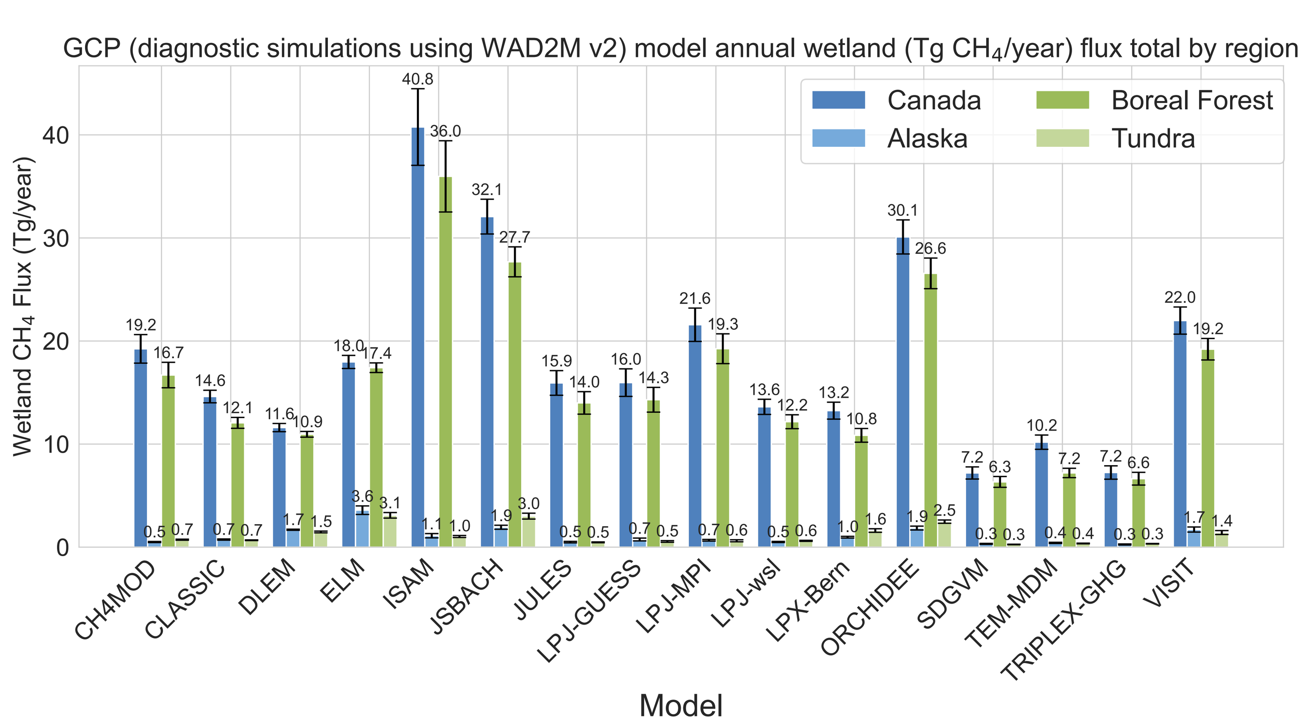

Figure 1. The 16 Global Carbon Project (GCP) global CH_4 wetland flux models that we use in the study.

STILT FOOTPRINTS

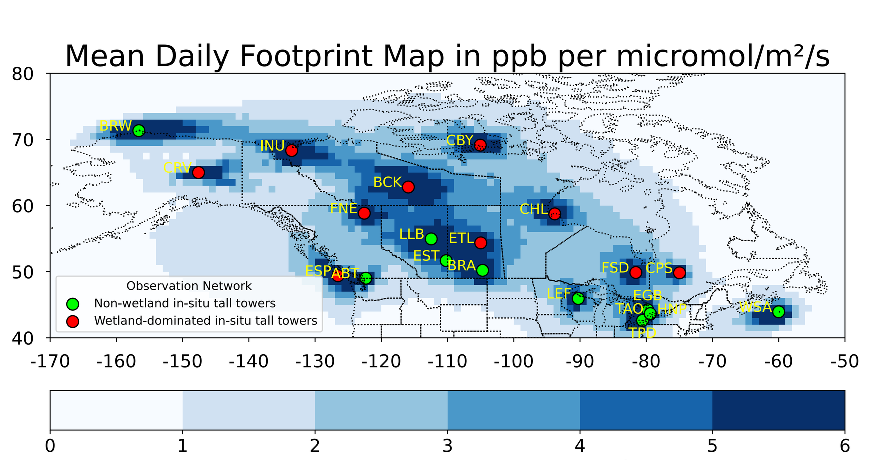

General form : Z ~ H[s + A + B] + b

- Z = Observation (n x 1)
- H = Influence Matrix (footprint)
- s = GCP wetland CH_4 flux estimates (m x 1)
- A = Anthropogenic CH_4 flux estimates (n x 1)
- B = Biomass burning CH_4 flux estimates (n x 1)
- b = Boundary condition (n x 1)

Figure 2. The US and Canadian atmospheric CH_4 observing network from 2007-2017. The figure also shows the WRF-STILT mean daily footprint map in ppb μmol^{-1} m^{-2} s^{-1} across the study domain of 40°N to 80°N and 170°W to 50°W. The lime-colored dots represent non-wetland sites, where the wetland-to-anthropogenic CH_4 concentration ratio is less than 1.5 (using anthropogenic emissions from the CAMS product). In contrast, the red-colored dots indicate wetland-dominated sites, where this ratio exceeds 1.5.

ATMOSPHERIC OBSERVATIONS FROM IN SITU TOWERS

- This study compares CH_4 flux models over a decade (2007-2017) using in-situ tower observations from Environmental Canada and NOAA in high-latitude north America regions.

High–latitude North America Biomes

Wetland-dominated sites by Biomes

Tundra: Carbon in Arctic Reservoirs Vulnerability Experiment (CRV); Cambridge Bay, Nunavut Territory (CBY).

Boreal Forests/Taiga: Inuvik, Northwest Territories (INU); Behchoko, Northwest Territories (BCK); Churchill, Manitoba (CHL); Fort Nelson, British Columbia (FNE); East Trout Lake, Saskatchewan (ETL); Fraserdale, Ontario (FSD); Chapais, Quebec (CPS).

Temperate Forests: Estevan Point, British Columbia (ESP)

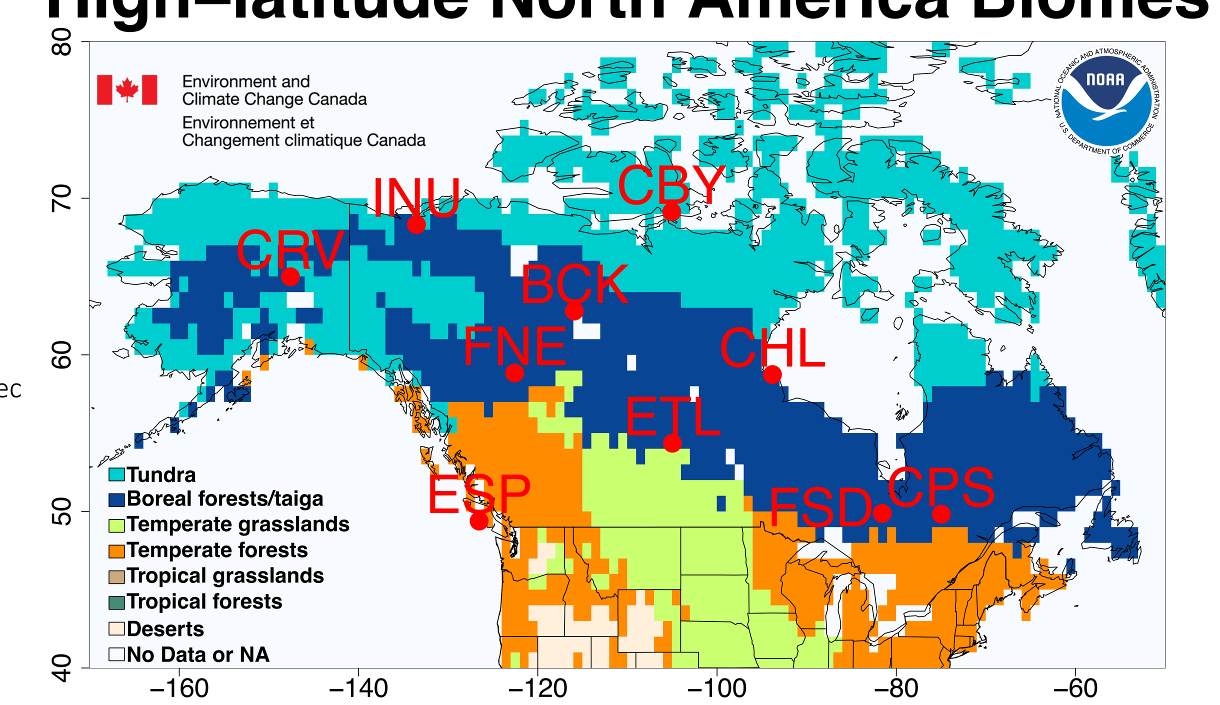

Figure 3. Biome map of high-latitude North America highlighting the four out of seven biome types examined in this study.

COMPARISONS WITH THE WETCHIMP MODELS

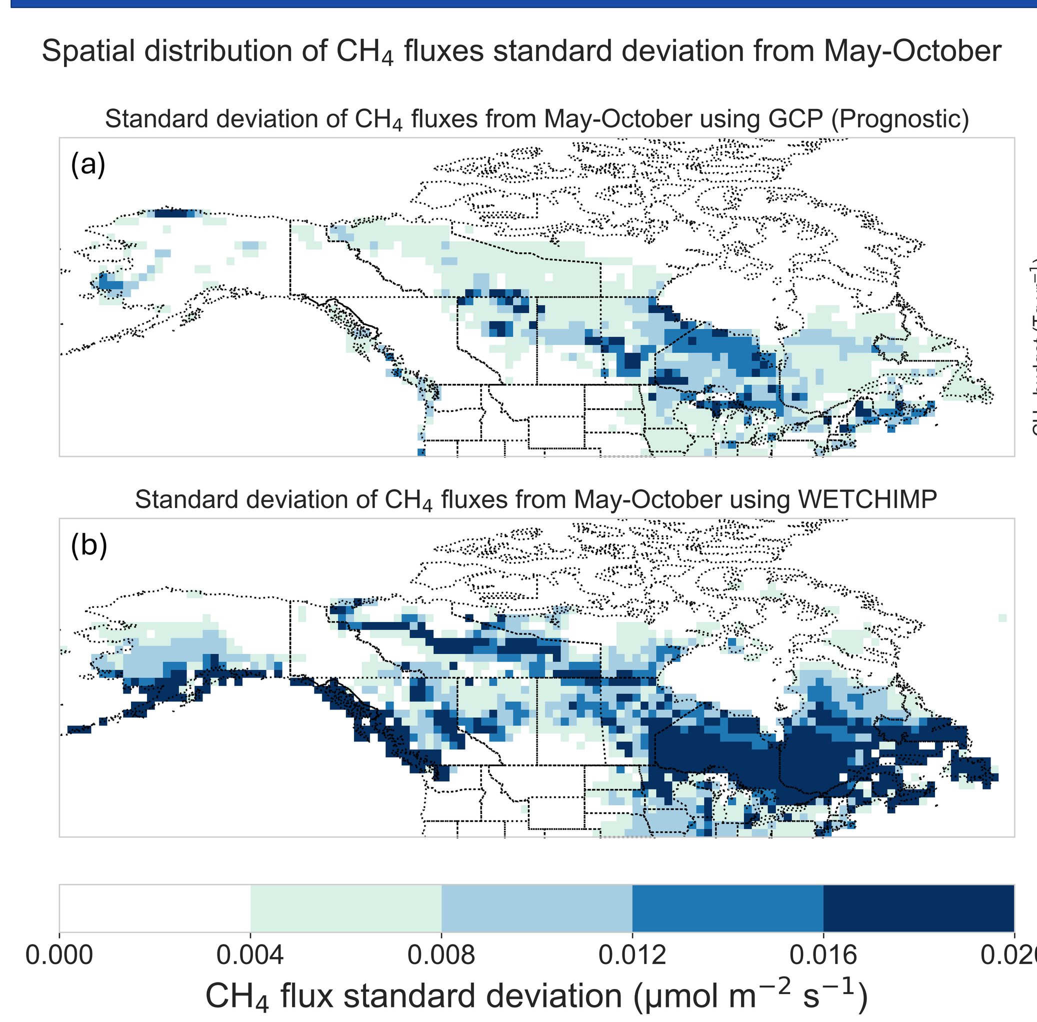

Figure 4. The inter-model standard deviation for each individual model grid box, calculated using the 11 prognostic GCP models (top) and WETCHIMP models (bottom). The inter-model uncertainty in model locations is higher for the WETCHIMP models than the GCP models. All fluxes have units μmol m^{-2} s^{-1}.

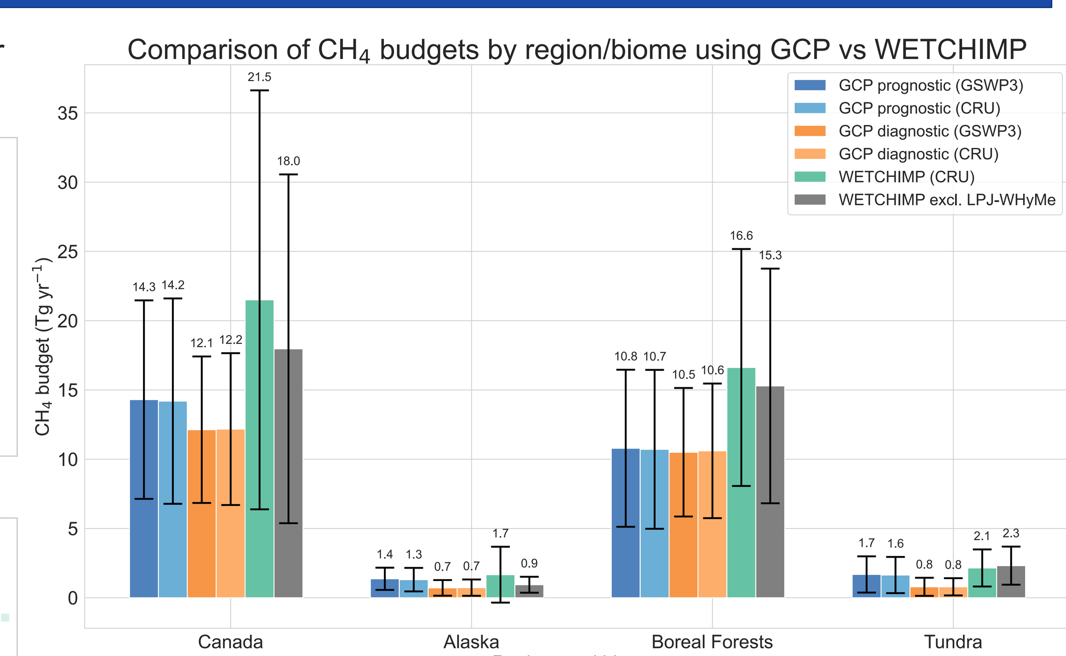

Figure 5. Annual CH_4 flux totals across Canada, Alaska, and several biomes. The four bars on the left of each region or biome represent the 2 different climate forcing data (GSWP3 and CRU) and prognostic versus diagnostic types for the GCP models. The green bar shows the mean annual CH_4 flux total using all WETCHIMP models, and the gray bar denotes the mean flux total excluding the ORCHIDEE model.

- ❖ CH_4 flux estimates from the GCP models are a factor of ~1.5 smaller across most of high-latitude North America compared to the WETCHIMP models.
- ❖ CH_4 fluxes estimated by the prognostic GCP models result in much lower inter-model uncertainty compared to the seven WETCHIMP models, with smaller inter-model disagreement across Canada and southern Alaska.

COMPARISONS WITH ATMOSPHERIC DATA

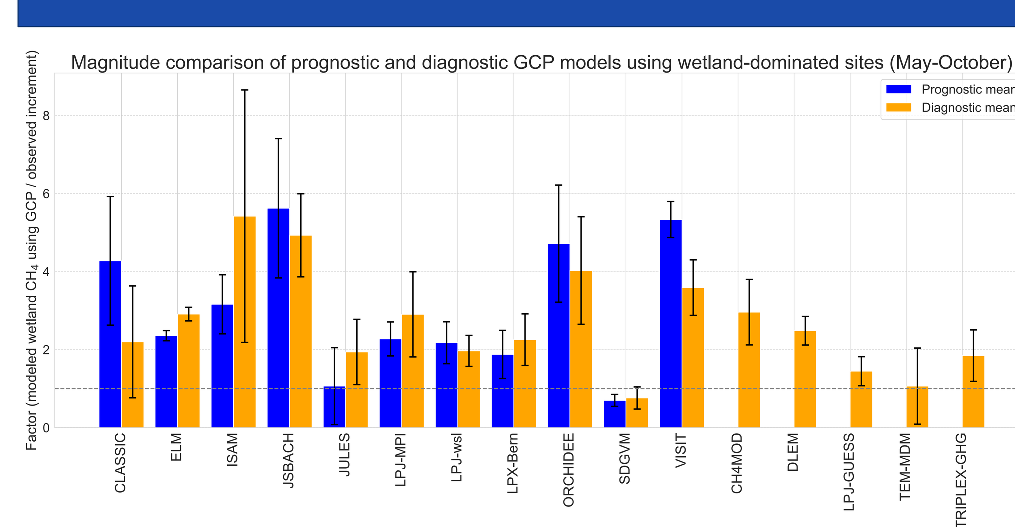

Figure 6. Comparisons between modeled mixing ratios from STILT against observations at the tower sites. The y-axis has values range from 0 to 9, representing the ratio between the modeled wetland CH_4 mixing ratios using the GCP models and the observed increment. We define the observed increment as the difference between atmospheric CH_4 observations and the sum of the boundary CH_4 levels, modeled anthropogenic CH_4 mixing ratios, and modeled biomass burning CH_4 mixing ratios.

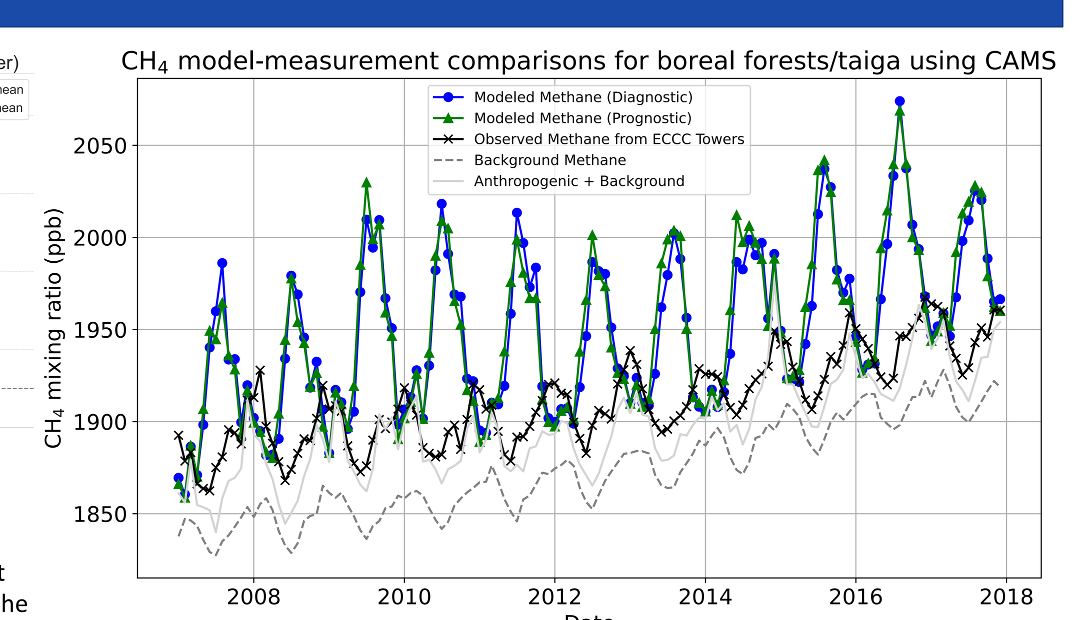

Figure 7. A time series of the mean modeled CH_4 mixing ratios using the STILT model with anthropogenic fluxes from CAMS and wetland fluxes set at the mean of the GCP ensemble across boreal forests/taiga using ten wetland dominated sites between 2007 and 2017.

COMPARISONS WITH ATMOSPHERIC DATA

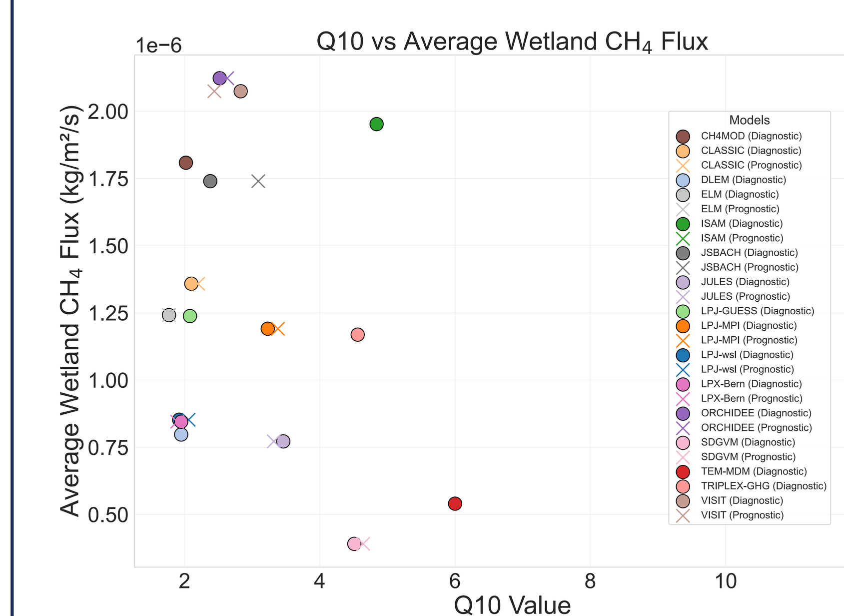

Figure 10. Q_{10} factors estimated for each of the GCP models. The plot also shows the relationship between the magnitude of fluxes estimated by each model for the study domain and the Q10 value estimated for each model.

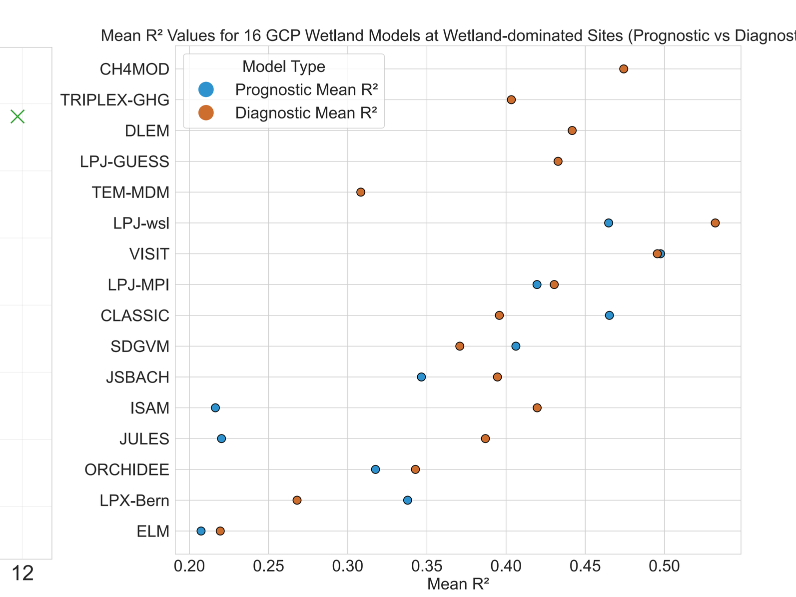

Figure 9. The correlation R^2 between modeled CH_4 mixing ratios using the GCP models and atmospheric observations. The y-axis lists all the prognostic and diagnostic GCP models, and x-axis shows the R^2 range for these GCP models.

SHARED SPATIAL-TEMPORAL PATTERNS

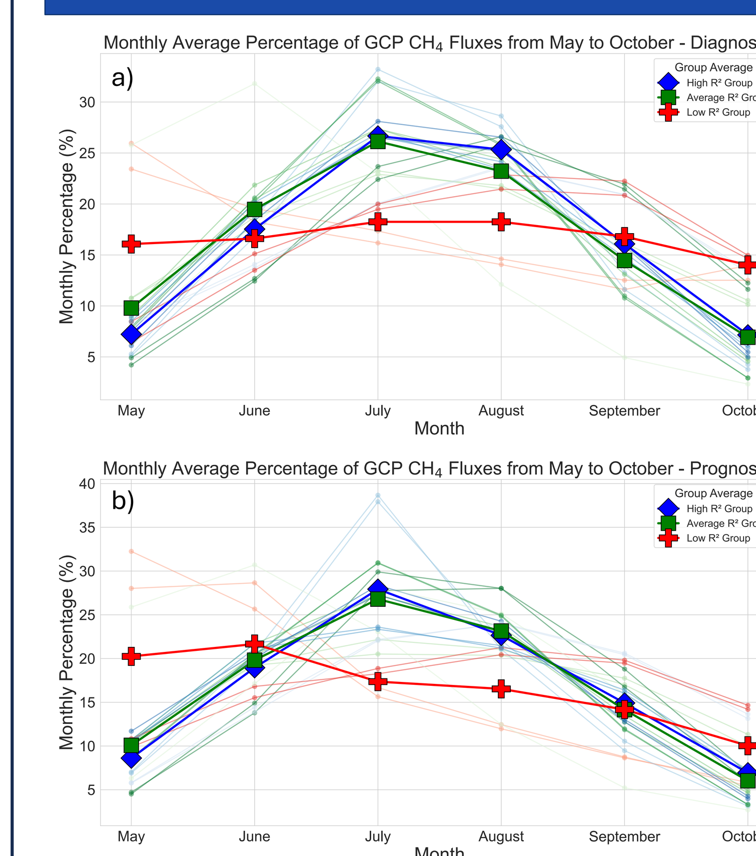

Figure 10. The seasonal cycles of the diagnostic GCP models (a) and prognostic GCP models (b) from 2007-2017. The blue, green, and red lines each represent the GCP models that have the highest, average, low R2 values with atmospheric observations. The x-axis represents the months from May to October throughout 2007-2017, and y-axis denotes the percentages of CH_4 fluxes that occur within that month.

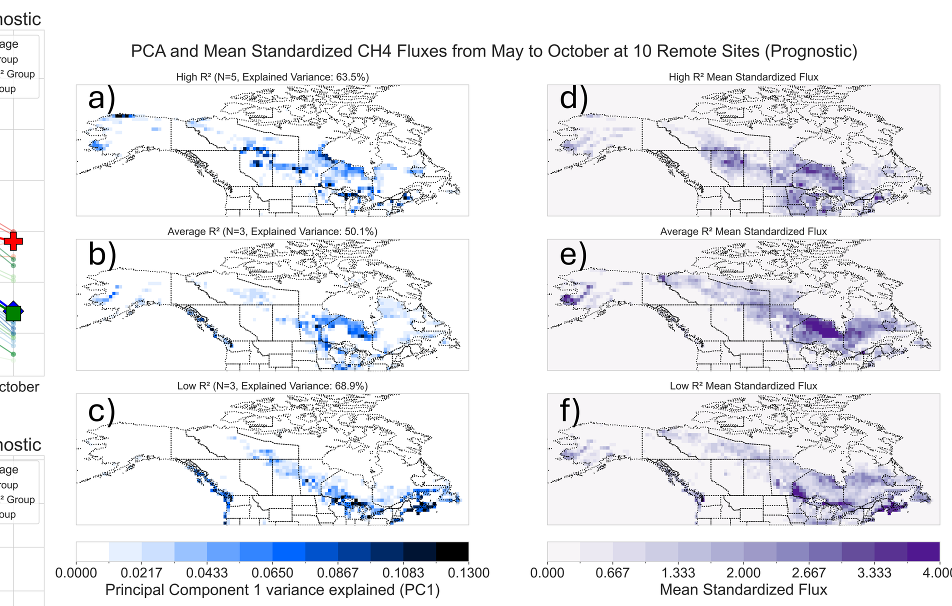

Figure 11. The PCA results and mean standardized CH_4 fluxes for the prognostic GCP models, run separately for each group of models – the high (a and d), average (b and e), and low (c and f) R^2 groups. .

- ❖ GCP models (with prognostic simulations) more consistent with atmospheric observations have a distinct seasonal peak in wetland CH_4 fluxes in July and August. In contrast, models that do not agree well with atmospheric observations have a flatter seasonal cycle.
- ❖ GCP models that run prognostically are most consistent with atmospheric observations concentrate their fluxes near the Hudson Bay Lowlands (HBL).

CONCLUSIONS

- ❖ GCP models have a much smaller flux magnitude and lower inter-model uncertainty across North America compared to a previous model inter-comparison (WETCHIMP).
- ❖ Process-based CH_4 models that are most consistent with atmospheric observations exhibit the highest percentage of fluxes in July and August relative to other months and have a sharper seasonal cycle. These models also concentrate fluxes near the HBL compared to the less skilled ones.
- ❖ Overall, we argue that the bottom-up modeling community had made large strides in reducing inter-model uncertainties, and these improvements are consistent with atmospheric CH_4 observations, yet there is still an enormous need for further improvements in these models.

Acknowledgements: This work is funded by the NASA ABoVE program. We thank collaborators at the NASA Global Monitoring Laboratory and Environment and Climate Change Canada. We also thank Ben Poulter, Zhen Zhang, and the CH_4 modeling groups involved in the Global Carbon Project. We thank ECCC and NOAA for their data support on in situ tower measurements across Canada and Alaska. We thank Leyang Feng, Ziting Huang, Mingyang Zhang, Dylan Gaeta, and Ao Chen from Johns Hopkins University.